Chaotic and phase-locked breather dynamics in the damped and parametrically driven sine-Gordon equation

Rainer Grauer and Yuri S. Kivshar*,†
Institut für Theoretische Physik I, Heinrich-Heine-Universität Düsseldorf, D-40225 Düsseldorf, Germany
(Received 11 June 1993)

The dynamics of a breather in the damped and parametrically driven sine-Gordon equation is investigated both numerically and analytically. The Kahunen-Loève expansion is applied to extract the energetically dominant localized modes. These modes are used in a Galerkin approximation to the original partial differential equation. The solutions of the resulting amplitude equations are then compared to numerical simulations of the perturbed sine-Gordon equation showing a perfect agreement. In addition, two collective-coordinate models (based on a direct approach and on the inverse-scattering transform) are constructed and their limitations in comparison with the Kahunen-Loève expansion and direct simulations are discussed. Finally, information from the periodic spectral theory and linear stability analysis is used to identify the Kahunen-Loève modes and to show why this approach gives rather good results.

PACS number(s): 03.40.Kf, 05.45.+b, 75.30.Ds

I. INTRODUCTION

As is well known, the sine-Gordon (SG) model is used to describe many physical effects in a one-dimensional approximation, for example, flux propagation in long Josephson structures, edge dislocations in crystals, nonlinear spin waves in superfluid A and B phases of ^{3}He, domain walls in ferro- and antiferromagnetic systems, etc. The elementary nonlinear localized excitations of the system are divided into two different classes, namely, *kinks* and *breathers*. The kinks describe statics and dynamics of topological excitations, like flux quanta (fluxons) in long Josephson junctions or domain walls in magnetic systems (see, e.g., the review paper [1] and references therein). The other type of soliton excitations, the so-called breathers, may be considered as dynamical bound states of kink-antikink pairs, with the nonlinear frequency lying within the gap of the linear spectrum.

In various applications the SG model is considered to be perturbed by an applied external field which, in particular, is periodic in time (see, e.g., Ref. [1]). When an ac (direct) forcing is applied to a SG breather, it can compensate for the dissipative losses and maintain a phase-locked stationary mode [2,3]. This effect has the same physical origin as the phase-locking of an envelope soliton described by an ac driven nonlinear Schrödinger (NLS) equation [2]. More detailed investigations of the ac driven damped SG system reveal complicated nonlinear dynamics including period doubling, spatial-temporal complexity, and chaos [4,5], and many of these phenomena have been well understood with the help of simplified dynamical models (see, e.g., Ref. [5]).

In a number of physically important nonlinear systems, e.g., magnetic systems [6,7], or long Josephson junctions [8,9], the applied periodic force acts *parametrically*, i.e., it varies parameters of the model. As is well known, physical effects produced by direct and parametric ac forces are rather different, e.g., in linear models oscillation instability due to a parametric force cannot be limited by applying dissipation, as it is in the case of a resonance produced by a direct ac force [10]. A similar difference may also be noted analyzing nonlinear resonances produced by both the ac forces [10]. As for soliton-bearing nonlinear systems, resonant input power related to the applied direct or parametric ac forces may lead to similar dynamical effects for both the driven models, e.g., a parametric force applied to the SG system may also support a phase-locked breather oscillation if the force amplitude exceeds a certain threshold value [11], the effect being qualitatively similar to the breather stabilization by a direct forcing in the damped SG system [3]. In the small-amplitude limit the parametrically driven damped SG model may be reduced to an effective nonlinear Schrödinger equation [11] (similar to the case of a direct forcing [2,12]) which supports exact localized solutions describing the phase-locked solitons [11,13] (cf. [14]).

Nevertheless, the different physical nature of the direct and parametric ac forces may show *very different scenarios of spatiotemporal complexity* in a driven nonlinear model with loss. It is a purpose of this paper to give a detailed analysis of the dynamics of the SG breather under the influence of an external *parametric* force, including the phase-locked regime of the breather oscillations, period-doubling and quasiperiodicity leading to a strange attractor.

The paper is organized as follows. In the next section, Sec. II, we briefly describe the model and its physi-

*Also at the Institute for Low Temperature Physics and Engineering, 310164 Kharkov, Ukraine.
†Present address: Optical Sciences Center, The Australian National University, ACT 2601 Canberra, Australia.

cally relevant applications. The bifurcation scenarios obtained from direct numerical simulations of this model are discussed in Sec. III. In the following two sections, Secs. IV and V, we analyze two types of simplified low-dimensional models described by ordinary differential equations. To construct the first model in Sec. IV we extract from the numerically obtained solutions of the perturbed SG equation the energetically most dominant localized modes by making use of the so-called Kahunen-Loève expansion [15,16]. With those modes as ansatz functions we perform a Galerkin projection of the perturbed SG equation. The second type of model uses a collective-coordinate ansatz (see, e.g., Refs. [17–24]) which allows adiabatic change of the breather parameters. In fact, in Sec. V we use two such models; the first one is based on the so-called direct approach, and the second one is derived with the help of the inverse-scattering transform. At last, in Sec. VI we try to understand why low-dimensional models (and, especially, the Kahunen-Loève expansion) work so well for this particular problem. One main indication is obtained from the periodic spectral theory applied to the numerically found solutions. As in the case of a direct ac forcing [5], the periodic spectral theory allows one to identify the various kinds of excitations composing the localized solutions. As we point out in Sec. VI, the case of a parametric driving is quite different from that of a direct driving. After having identified the dominant excitations we make a linear stability analysis of small-amplitude solutions around the breather with the help of the linearized Bäcklund transformation (see, e.g, Ref. [17]). Having the information so far, it is then not astonishing that the Kahunen-Loève modes can be identified with the breather and the linear modes around the breather. Section VII concludes the paper.

II. MODEL

The model we deal with in the present paper is described by the damped and parametrically driven SG equation

$$u_{tt} - u_{xx} + \sin u = -\alpha u_t + \Gamma \sin(\omega t) \sin\left(\frac{u}{n}\right) , \qquad (1)$$

where Γ and α stand for the strength of the parametric forcing and damping, respectively. The frequency ω is assumed to be selected within the region where linear waves are stable to the parametric forcing, i.e., $\omega/2 < \omega_m$, $\omega_m = 1$ being the gap of the linear spectrum of the unperturbed SG equation.

Equation (1) may be derived, for example, as an effective equation of motion for the magnetization vector in several magnetic models, u being the angle describing the orientation of the magnetic vector in a selected (e.g., easy anisotropy) plane. The perturbation from the right-hand side (rhs) of Eq. (1) appears if one considers the variable magnetic field [25,26]. Another physically relevant example of Eq. (1) with $n = 1$ is a long Josephson junction with parametrically varying critical current (see Refs. [8,27,9]).

For simplicity, in the present paper we consider the case when $n = 2$, but many conclusions of the present analysis may also be extended in a straightforward manner to cover a more general case (see, e.g., Ref. [11] where a similar generalization has been made for the breather stabilization problem). The model (1) with $n = 2$ exactly corresponds, e.g., to a weak two-sublattice ferromagnetic (antiferromagnetic) system [26]. In that case the main nonlinearity ($\sim \sin u$) is caused by the magnetic anisotropy, and the parameter Γ is proportional to the amplitude of the external (variable) magnetic field.

In the absence of any perturbations, i.e., for $\Gamma = \alpha = 0$, Eq. (1) is exactly integrable and it has two different types of soliton solutions, kinks and breathers. Existence of kinks is a general property of many nonlinear systems with degeneracy of the ground state. However, breathers are more special objects which in fact may be found as exact solutions in integrable models. The breather at rest has the form

$$u_{\rm br}(x,t) = 4\tan^{-1}\left[\frac{\sqrt{1-\omega_{\rm br}^2}}{\omega_{\rm br}} \frac{\sin(\omega_{\rm br} t + \theta)}{\cosh[x\sqrt{1-\omega_{\rm br}^2}]}\right] , \qquad (2)$$

$\omega_{\rm br}$ being the breather frequency, $0 < \omega_{\rm br} < 1$, and θ is an arbitrary initial phase. The moving breather may be obtained from Eq. (2) by a Lorentz transformation.

III. NUMERICAL SIMULATION RESULTS

Equation (1) is integrated with periodic boundary conditions

$$u\left(x = -\frac{L}{2}\right) = u\left(x = \frac{L}{2}\right) . \qquad (3)$$

We consider a rather long system length, $L = 80$, and choose the resonant breather frequency $\frac{\omega}{2}$ to lie within the gap, in particular, in the range 0.90–0.98. The damping is fixed to $\alpha = 0.004$ and Γ is varied as a *bifurcation parameter*.

While increasing the amplitude Γ of the driving force, the first stage of the bifurcation scenario is generic for all studied frequencies ω: at some critical Γ a stable phase-locked breather appears by a saddle-node bifurcation. Increasing the driving Γ results in a Hopf bifurcation. The bifurcation behavior hereafter depends on the driving frequency ω and the length L. For $\frac{\omega}{2} = 0.98$ a period-doubling sequence is observed, and it is shown in Fig. 1. We have obtained this result by integrating the perturbed SG equation (1) up to time 60 000 and throwing away the transient phase. Then we take two Poincaré sections of the data $(u(x=0), u_t(x=0))$ corresponding to the driving and the Hopf bifurcation frequency while the parameter Γ is varied. We observed that the period-doubling bifurcations occur either when the frequency $\frac{\omega}{2}$ goes to 1 for fixed L or for fixed ω letting the length L go to infinity. This behavior is similar to the ac-driven case studied in detail in Ref. [5]. For $\frac{\omega}{2} = 0.93$ and $\frac{\omega}{2} = 0.92$ we observe a transition to chaos by quasiperiodicity. First, a third frequency is observed. Finally, this

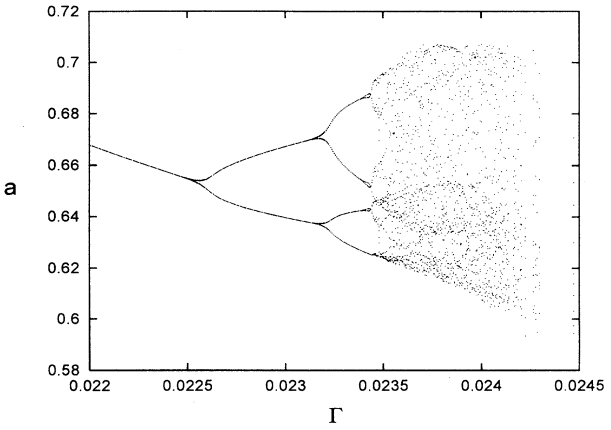

FIG. 1. Period-doubling sequence obtained for $L = 80$, $\alpha = 0.004$, $\omega = 1.96$ and varying Γ. The quantity a stands for the value of $u(x = 0)$ in the second Poincaré map.

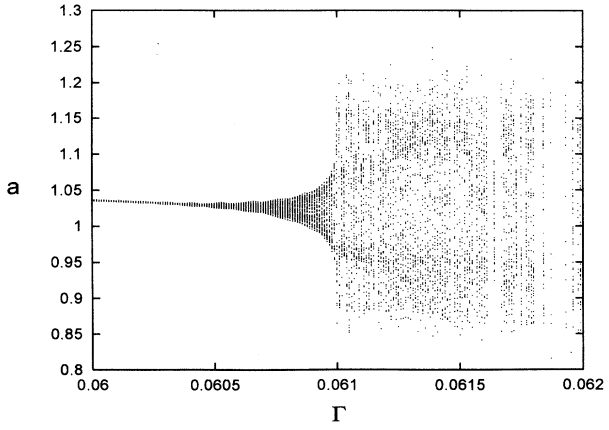

FIG. 3. Transition from quasiperiodicity to chaotic motion for $L = 80$, $\alpha = 0.004$, $\omega = 1.84$.

three-frequency torus becomes unstable and we have the Ruelle-Takens way to chaos (see, e.g., [28]). This behavior is depicted in Figs. 2 and 3.

The upshot of the numerical investigations is as follows: (i) we see various bifurcations of a *single* breather; (ii) letting the system length L go to infinity, only the period-doubling route can be observed.

In the next sections we try to develop low-dimensional models which can be responsible for the scenarios observed in numerical simulations. Since the collective-coordinate models analyzed below (Sec. V) take as a basis a breather for an infinite system, we only concentrate on the regime of large system lengths L where only period doubling has been observed.

IV. THE KAHUNEN-LOÈVE EXPANSION

In this section we apply the Kahunen-Loève expansion to the numerically obtained solutions. The Kahunen-Loève expansion [15] has quite a long history, going even back to the last century according to [29]. The method was first applied to fluid turbulence by Lumley [30,16] and got a lot of attention in the dynamical systems community since the work of Aubry *et al.* [31].

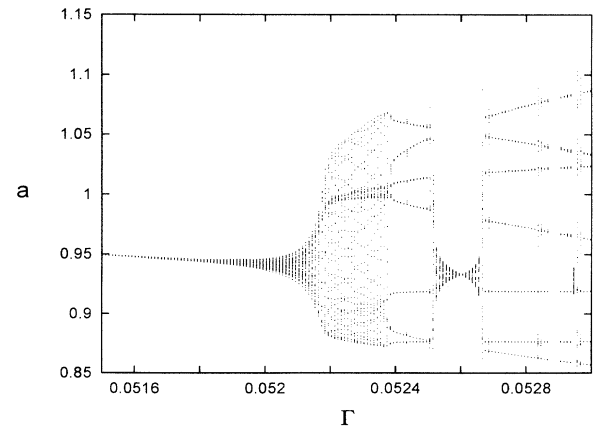

FIG. 2. Transition from quasiperiodicity to chaotic motion for $L = 80$, $\alpha = 0.004$, $\omega = 1.86$.

In application to the problem under consideration, the method consists in formulating the linear eigenvalue problem

$$\int_{-\frac{L}{2}}^{\frac{L}{2}} \mathcal{K}(x,x')\phi_n(x')\,dx' = \lambda_n \phi_n(x) \ , \tag{4}$$

where the two-point correlation function $\mathcal{K}(x,x')$ is defined by the time average

$$\mathcal{K}(x,x') = \lim_{T\to\infty} \frac{1}{T} \int_0^T u(x,t)u(x',t)\,dt \tag{5}$$

and $u(x,t)$ is a solution of the perturbed SG equation (1). The orthonormal functions ϕ_n are called *empirical eigenfunctions*, and in our case they are obtained from the numerical solutions of Eq. (1). To be more specific, we integrate Eq. (1) up to time 10 000. For our parameters ($\alpha = 0.004$, $\omega \approx 1.96$, and $\Gamma \approx 0.025$) the asymptotic regime is already reached about time 3000. To build the correlation function $\mathcal{K}(x,x')$ we use 1000 samples in the time interval between 5000 and 10 000.

The useful property about the empirical eigenfunctions ϕ_n is that they are the optimal choice for a Galerkin approximation. If we define the projection $\mathcal{P}_N$ onto the first N eigenfunctions as the following,

$$\begin{aligned} \mathcal{P}_N[u(x,t)] &= \textstyle\sum_{n=1}^{N} a_n(t)\phi_n(x) \ , \\ a_n(t) &= \textstyle\int_{-\frac{L}{2}}^{\frac{L}{2}} u(x,t)\phi_n(x)\,dx \ , \end{aligned} \tag{6}$$

then it is easy to show that the eigenfunctions ϕ_n minimize the error $\langle ||\mathcal{Q}_N u||_2 \rangle$ for every N, where the brackets $\langle\ \rangle$ denote the time average, $||\ ||_2$ stands for the L_2 norm, and $\mathcal{Q}_N = 1 - \mathcal{P}_N$. This directly implies that they are ordered with respect to the energy. They also minimize the representational entropy S (see Ref. [32])

$$S = -\sum_{n=1}^{N} \frac{a_n}{\langle ||u||_2 \rangle} \ln \frac{a_n}{\langle ||u||_2 \rangle} \tag{7}$$

which is a consequence of the former property.

The first nine eigenfunctions are displayed in Fig. 4. The first one has simply the shape of the breather itself. The higher modes look like radiation modes *modified* by the breather. We come back to the discussion of the physical meaning of the modes in Sec. VI.

The next step is to use the eigenfunctions ϕ_n in a Galerkin approximation

$$\mathcal{P}_N \Bigg[\partial_{tt} u - \partial_{xx} (\mathcal{P}_N u) + \sin(\mathcal{P}_N u) + \alpha u_t + \Gamma \sin(\omega t) \sin\left(\mathcal{P}_N \frac{u}{2}\right) \Bigg] = 0 \ . \tag{8}$$

In order to solve Eq. (8), we approximate the sine function by a Chebyshev polynomial

$$\sin(u) \approx c_1 u + c_2 u^3 \ , \quad c_1 = 0.997\,481\,295\,4 \ , \quad c_2 = -0.156\,506\,831\,9, \tag{9}$$

so that the maximal error between $-1 < u < 1$ is less than 2×10^{-2}.

The surprising fact is that only *two* modes are in fact necessary to pick up the essential properties of the perturbation-induced breather dynamics of the parametrically driven damped SG breather described by Eq. (1). To support such a statement, in Fig. 5(a) we show the Poincaré map of the phase space $(u, \dot{u})$ where the coordinates are computed by projecting the numerically obtained partial differential equation (PDE) solutions onto the first eigenfunction. Figure 5(b) instead is obtained from the Galerkin approximation making use only of two modes. The error in the location of the bifurcation points is less then 4%.

V. COLLECTIVE-COORDINATE ANALYSIS

A. A direct approach

There are several variational methods to obtain reduced evolutional equations describing the perturbation-induced breather dynamics. One of those methods is based on a Lagrangian (Hamiltonian) formalism and in its simplest form the method was proposed in [20] (see

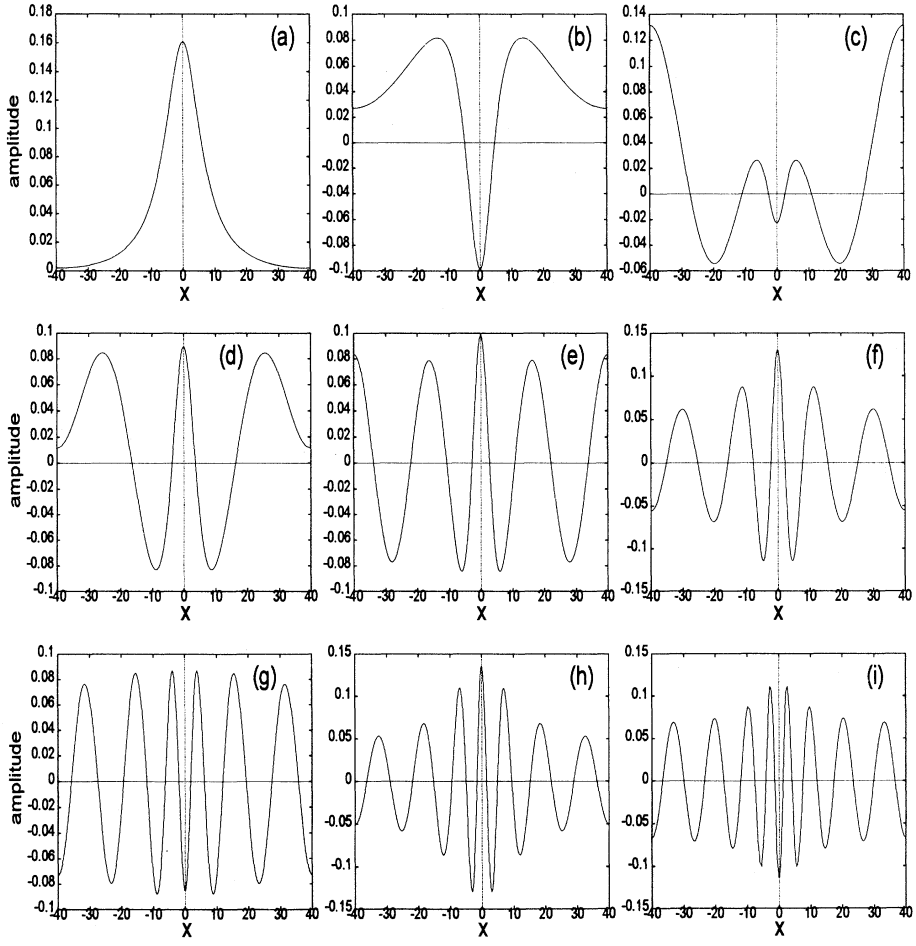

FIG. 4. The first nine empirical eigenfunctions obtained from from the direct simulation for $L = 80$, $\alpha = 0.004$, $\omega = 1.96$, and $\Gamma = 0.023$.

also [22]). The main basis of any variational approach is to select a proper ansatz. The choice of the ansatz may allow one to remove singularities which frequently occur in the system of the corresponding ordinary differential equations (ODE's) resulting from that ansatz (see, e.g., [23]).

Following [20] (see also [22]), we use for a breather in a parametrically perturbed SG equation (1) the following ansatz:

$$u_{\rm br}(x,t) = 4\tan^{-1} e^{k(x+z)} - 4\tan^{-1} e^{k(x-z)} \equiv 4\tan^{-1}\left[\frac{\sinh(kz)}{\cosh(kx)}\right], \tag{10}$$

which is in fact a linear superposition of a kink and antikink. For the kink (antikink) in the pure SG equation, one would have $k \equiv (1-\dot{z}^2)^{-1/2}$ and $\dot{z} \equiv dz/dt = \text{const}$ while the breather would be determined by the relation [see Eq. (2)]

$$\sinh[kz(t)] = \frac{k}{\omega_{\rm br}} \sin(\omega_{\rm br} t + \theta), \tag{11}$$

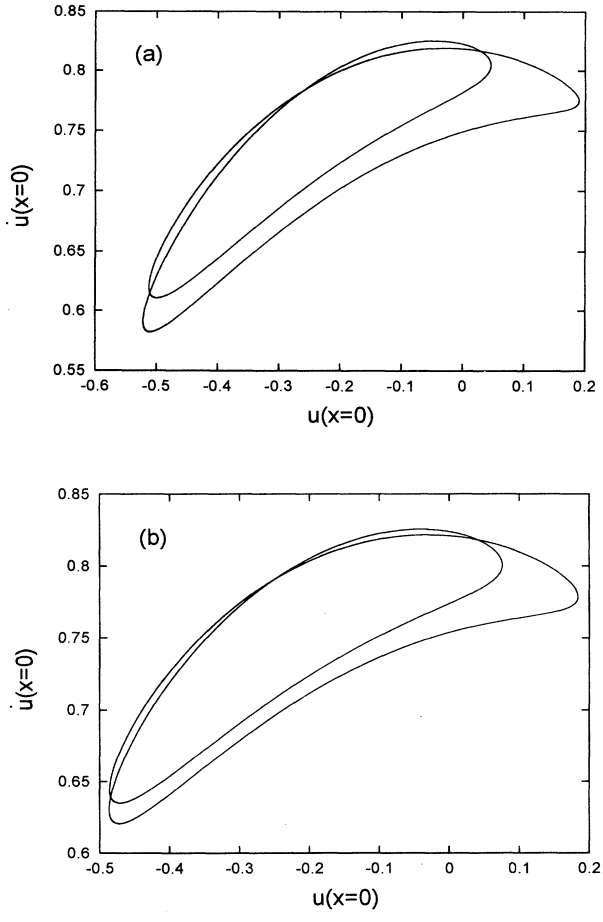

FIG. 5. The phase space of the first Kahunen-Loève mode obtained (a) from numerical solution of Eq. (1) and (b) from the two-mode Galerkin expansion.

with $\omega_{\rm br} = \sqrt{1-k^2}$. Let us now consider Eq. (10) as an *ansatz* in the system Lagrangian density defined as

$$L = \int_{-\infty}^{\infty} dx \left\{ \frac{1}{2}u_t^2 + \frac{1}{2}u_x^2 - (1-\cos u) + 2\Gamma \sin(\omega t)[1-\cos(u/2)] \right\}. \tag{12}$$

If we assume $\dot{k} = 0$, then the parameter $z(t)$ is the only effective variable, and its evolution is determined by the effective Lagrangian density,

$$L = \tfrac{1}{2}M(z)\dot{z}^2 - U(z) + L_p(z), \tag{13}$$

where the dot means time derivative, and

$$M(z) = 16k\left[1 + \frac{2kz}{\sinh(2kz)}\right], \tag{14}$$

$$U(z) = \frac{M(z)}{2k^2}\tanh^2(kz) - \tfrac{1}{2}M(z) + 16k, \tag{15}$$

$$L_p(z) = 4\Gamma \sin(\omega t) z \tanh(kz). \tag{16}$$

Dissipation-induced effects in the effective collective-coordinate model may be taken into account calculating the dissipative function, $Q = \frac{1}{2}\int dx u_t^2$, which for the variable $z(t)$ takes the form

$$Q = \tfrac{1}{2}\alpha M(z)\dot{z}^2. \tag{17}$$

Equations (13)–(17) define the dynamics of an effective particle with the coordinate $z(t)$ and a variable mass $M(z)$, which is described by the motion equation,

$$\frac{d}{dt}\left[M(z)\dot{z}\right] = \tfrac{1}{2}M'(z)\dot{z}^2 - U'(z) + L_p'(z) - \alpha M(z)\dot{z}, \tag{18}$$

where the primes stand for the derivatives in z.

B. Perturbation theory based on the inverse-scattering transform

The perturbation theory based on the inverse-scattering transform (IST) is a rather well developed approach, and it uses the fact that the pure SG model is exactly integrable (see, e.g., Ref. [1] for an extended review). The main idea of the method is to use the IST technique to derive evolutional equations for the soliton (in particular, breather) parameters. This method also assumes a choice of an ansatz, but such an ansatz is usually taken in the simplest form, just using an exact breather shape with the parameters being assumed to be defined later on. In the case of the SG equation, it is convenient to take the perturbed breather in the form

$$u_{\rm br}(x,t) = 4\tan^{-1}\left[\frac{\sqrt{1-\omega_{\rm br}^2}}{\omega_{\rm br}}\frac{\sin\chi}{\cosh(x\sqrt{1-\omega_{\rm br}^2})}\right], \quad (19)$$

where the breather's frequency $\omega_{\rm br}$ and the phase derivative $\dot{\chi}$ are assumed to be slowly varying in time. Equations to describe evolution of χ and $\omega_{\rm br}$ in the presence of the parametric forcing and damping are derived by means of the IST method (see, e.g., [1]) from the general equations given in the Appendix, and they may be written in the form

$$\dot{\omega}_{\rm br} = -(1-\omega_{\rm br}^2)\cos\chi H(\omega_{\rm br},\chi)[1+I(\omega_{\rm br},\chi)], \quad (20)$$

$$\dot{\chi} = \omega_{\rm br} - \frac{\sin\chi}{\omega_{\rm br}}H(\omega_{\rm br},\chi)[1+(1-\omega_{\rm br}^2)\cos^2\chi I(\omega_{\rm br},\chi)]. \quad (21)$$

Here we have introduced the notations

$$H(\omega_{\rm br},\chi) = \frac{[\frac{1}{2}\Gamma\sin(\omega t)\sin\chi - \alpha\omega_{\rm br}\cos\chi]}{[\omega_{\rm br}^2 + (1-\omega_{\rm br}^2)\sin^2\chi]}, \quad (22)$$

$$I(\omega_{\rm br},\chi) = \frac{1}{a\sqrt{a^2+1}}\ln\left(\frac{\sqrt{a^2+1}+a}{\sqrt{a^2+1}-a}\right), \quad (23)$$

where

$$a^2 \equiv \frac{1-\omega_{\rm br}^2}{\omega_{\rm br}^2}\sin^2\chi. \quad (24)$$

Equations (20)–(24) give a full set of the so-called adiabatic equations for the perturbation-induced dynamics of a SG breather at rest, and these equations are qualitatively consistent with one second-order differential equation (18) of the direct approach.

C. Comparison with numerical simulations

We have used the equations derived in the framework of the two collective-coordinate methods to compare the corresponding results with those given by direct numerical simulations. First of all, the collective-coordinate models can describe rather well the saddle-node bifurcation to a stable and unstable breather, but *both the approaches do not allow one to recover any further bifurcations.* It is not too surprising that the period-doubling sequence cannot be captured at this choice of the system parameters, since even for large amplitudes of order one the SG equation can be mapped to an effective nonlinear Schrödinger equation with the effect that the corresponding collective-coordinate models are only two dimensional equations which are first order in time. This result is valid for the ac periodic direct [12] as well as parametric [11] driving forces. This confirms the ansatz using the Kahunen-Loève modes which also take radiation modes into account.

Nevertheless, we would like to note that the onset of existence of the breather is much better described by Eqs. (20), (21) based on the IST approach. For example, the value of the threshold field amplitude to support the breather compared to that obtained from a direct numerical integration is indistinguishable, whereas the collective-coordinate equation (18) shows a deviation of about 25%.

VI. PERIODIC SPECTRAL THEORY AND LINEAR STABILITY ANALYSIS

Periodic spectral theory has successfully been used (see Refs. [33,5]) to identify the modes present in the system. The key to the method is that the unperturbed SG equation results as an integrability condition to the following differential equations (see, e.g., [34–36]):

$$\left[\begin{pmatrix}0&-1\\1&0\end{pmatrix}\frac{d}{dx} + \frac{i}{4}w\begin{pmatrix}0&1\\1&0\end{pmatrix} + \frac{1}{16\sqrt{E}}\begin{pmatrix}e^{iu}&0\\0&e^{-iu}\end{pmatrix} - \sqrt{E}\right]\Psi = 0, \quad (25)$$

$$\left[\begin{pmatrix}0&-1\\1&0\end{pmatrix}\frac{d}{dt} + \frac{i}{4}w\begin{pmatrix}0&1\\1&0\end{pmatrix} - \frac{1}{16\sqrt{E}}\begin{pmatrix}e^{iu}&0\\0&e^{-iu}\end{pmatrix} - \sqrt{E}\right]\Psi = 0\ , \quad (26)$$

where $w \equiv u_x + u_t$ and Ψ is a two dimensional vector.

In the case of periodic boundary conditions for u the search for bounded solutions of (25) defines an eigenvalue problem in $\lambda = \sqrt{E}$. This (continuous) spectrum consists of the real-λ axis plus spines connected to it and bands of the spectrum which lie in the complex plane. In Ref. [5] further details can be found as to how the spectrum may be numerically calculated.

In the integrable case the spectrum does not change in time and it is the central object of the integrable theory with periodic boundary conditions (see, e.g., [37–39]). Although the knowledge of the spectrum is not sufficient to reconstruct the solution u, the location of the bands already contains information about the spatial and temporal behavior of the solution. For example, spines connected to the real-λ axis correspond to radiation modes, bands on the imaginary axis to (anti-) kink trains whereas bands located on a circle of radius $r = 1/4$ belong to breather trains.

In Fig. 6 the spectrum for the perturbed SG equation (1) is shown for nine different times. The parameters are such that the dynamics is a period-2 motion. The sequence in Fig. 6 shows half of the period-2 cycle. Although the perturbed problem (1) is not integrable anymore the spectrum still gives us inside which modes are present in the system. In our case, the breather band changes adiabatically. Radiation modes, especially the $k = 0$ mode, are also excited. It is worth mentioning that

the radiation modes *are well separated from the breather band.* There is no colliding between the breather band and the spines. Therefore the complicated (and, especially, chaotic) SG breather dynamics cannot be caused by the occurrence of a double point as argued by [33] in the case of a direct driven force. Our explanation for the complicated nonlinear dynamics of the perturbed SG equation is very simple: one has to study the marginal modes around the breather. Only a few of them are effectively excited by the parametric driving, all others are damped and therefore slaved. The dynamics can then be described by an attractor consisting of a few modes, which can, in principle, be obtained by center-manifold theory.

To confirm this point of view we calculated the marginal modes for the unperturbed SG equation linearized around the breather $u_{\rm br}$ given by Eq. (2)

$$u_{tt} - u_{xx} + \cos(u_{\rm br})u = 0 \,, \tag{27}$$

u being assumed small in comparison with $u_{\rm br}$, and compared them to the Kahunen-Loève modes. Due to the integrability of the SG equation one can explicitly calculate all marginal modes as shown by McLaughlin and Scott [17]. To do this one makes use of a Bäcklund transformation to calculate from the radiation modes around the flat solution $u = 0$ the radiation modes around the kink (antikink). Using these modes the radiation modes around the breather can be calculated by applying the Bäcklund transformation once more again. The explicit formula for the solutions of Eq. (27) is

$$u_k(x,t) = \exp\left(\pm i\omega_k t + i\frac{2\pi}{L}kx\right)\left\{1 - \frac{\gamma}{\omega}\left(\frac{\cosh^2(\gamma x) - \sin^2(\omega t)}{\cosh^2(\gamma x) + \frac{\gamma^2}{\omega^2}\sin^2(\omega t)}\right)\left[\frac{\gamma\omega\lambda^2/2}{\lambda^4 + (\gamma^2-\omega^2)\lambda^2/8 + 1/16^2}\right.\right.$$
$$\left.\left. + i\frac{(\lambda^3 - \lambda/16)\omega\sinh(2\gamma x) - (\lambda^3 + \lambda/16)\gamma\sin(2\omega t)}{[\lambda^4 + (\gamma^2-\omega^2)\lambda^2/8 + 1/16^2][\cosh(2\gamma x) + \cos(2\omega t)]}\right]\right\} . \tag{28}$$

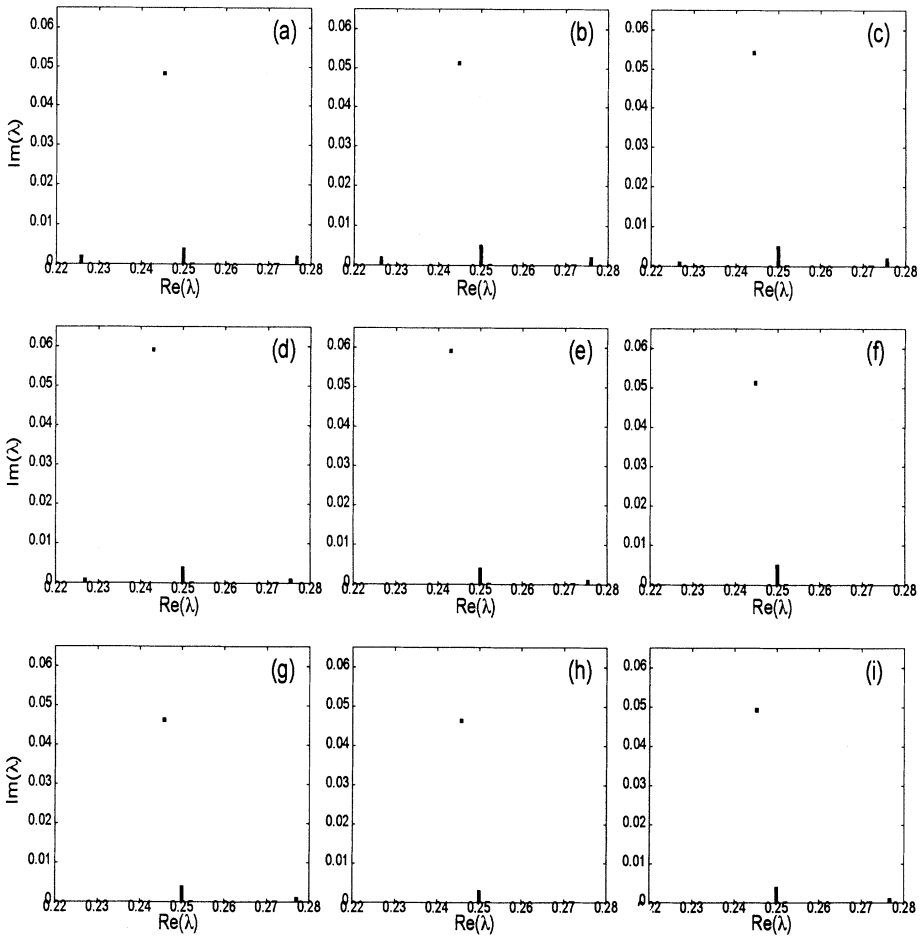

FIG. 6. Time evolution of the spectrum of Eq. (25) in the complex λ plane during half of a period-2 cycle.

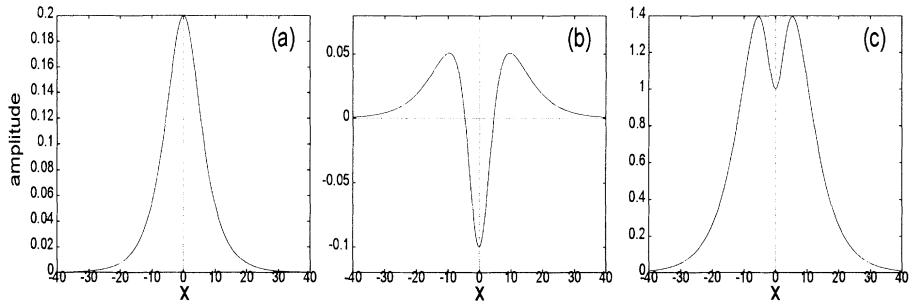

FIG. 7. The derivatives of the breather with respect to ω, t_0, and a combination of both.

In addition to these modes other solutions can be found by differentiation of the breather with respect to its parameters. In our spatially symmetric case we have the additional solutions of Eq. (27) defined as

$$\frac{\partial}{\partial\omega}u_{\rm br} = \frac{4}{1-\frac{\gamma^2}{\omega^2}\frac{\sin^2(\omega t)}{\cosh^2(\gamma x)}}\left[\frac{-1}{\gamma\omega^2}\frac{\sin(\omega t)}{\cosh(\gamma x)} + \frac{\gamma}{\omega}t\frac{\cos(\omega t)}{\cosh(\gamma x)} + \sin(\omega t)x\frac{\sinh(\gamma x)}{\cosh^2(\gamma x)}\right], \quad (29)$$

$$\frac{\partial}{\partial t_0}u_{\rm br} = -\left(\frac{4\gamma}{1+\frac{\gamma^2}{\omega^2}\frac{\sin^2(\omega t)}{\cosh^2(\gamma x)}}\right)\frac{\cos(\omega t)}{\cosh(\gamma x)}, \quad (30)$$

which correspond to change in frequency and temporal phase, respectively.

Figure 7 shows the modes (29),(30) and a combination of them whereas Fig. 8 shows the first six radiation modes. If one compares this figures with Fig. 4 for the modes following from the Kahunen-Loève expansion, one can see that the marginal modes and the Kahunen-Loève modes span similar subspaces.

VII. CONCLUSIONS

In conclusion, we have investigated the phase-locked and chaotic dynamics of the breather in a parametrically driven damped SG model numerically and by applying different collective-coordinate methods. We have shown that the bifurcation scenarios observed in numerical simulations may be explained in the framework of a collective-coordinate approach but the most perfect agreement has been achieved by using the Kahunen-Loève modes, i.e., those corresponding to a series of energetically most dominant localized modes of the forced breather oscillations. Here the Kahunen-Loève approach is applied to a soliton-bearing model and in the case analyzed here the method does show *excellent* agreement with direct numerical simulations in the framework of a corresponding PDE. In particular, as has been shown in the present study, only *two* modes of the Kahunen-Loève approach are in fact necessary to pick up the most essential properties of the phase-locked breather dynamics including a series of bifurcations and transition to chaos. One of the reasons why the method works so perfectly in comparison with a standard collective-coordinate approach has been shown by applying a linear stability

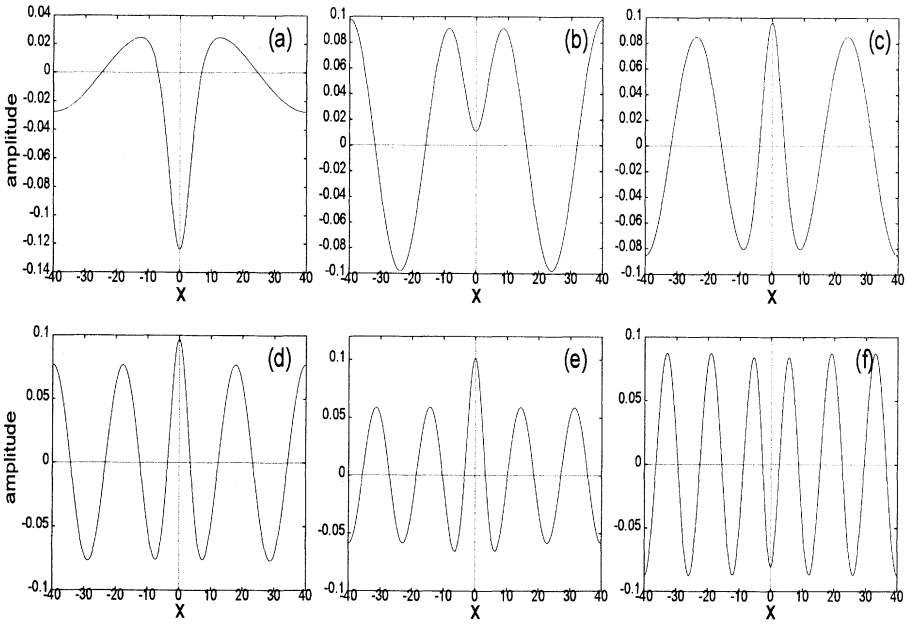

FIG. 8. The first six radiation modes [see Eq. (28)] around the breather.

analysis based on the Bäcklund transformation. Another reason is the nature of the ac force itself: A parametric driving force, being out of the parametric instability condition, does not excite a background as in the case of a direct ac forcing, so that the breather and radiation modes split to be detected in their "pure" form.

We believe the approach based on the energetically dominant Kahunen-Loève modes is one of the most effective approaches to describe driven and damped dynamics of localized modes (including solitonic ones as a particular case), so that the method can be widely used in a variety of different soliton-bearing models dealing with ac driven damped dynamics of nonlinear waves.

ACKNOWLEDGMENTS

The work of Yu. Kivshar was supported by the Alexander von Humboldt Stiftung. He is also indebted to Institut für Theoretische Physik I for a warm scientific atmosphere during the author's stay there.

APPENDIX

In this appendix we present the basic formulas of the perturbation theory based on the IST method applied to a SG breather. The results displayed below may be considered as a particular case of the formulas presented in [1] when the breather is at rest.

We start from the perturbed SG equation of the form

$$u_{tt} - u_{xx} + \sin u = \epsilon \mathcal{R}(u), \tag{A1}$$

where ϵ is assumed to be small and, for simplicity, $\mathcal{R} \to 0$ at $|x| \to \infty$ (otherwise, we should make a renormalization, see Ref. [1]). At $\epsilon = 0$ the SG equation (A1) may be subject to the IST method which consists in finding (discrete or continuous) spectral data of an auxiliary linear problem associated with the SG equation, the so-called scattering data defined for the initial conditions $u(x,0)$ and $u_t(x,0)$. The unperturbed temporal evolution of the scattering data is rather trivial, and the main subject of the IST method is to solve the so-called inverse-scattering problem which allows one to find the solution $u(x,t)$ with the help of the scattering data using their simple evolution in time. The main idea of the perturbation theory based on the IST is to use all the steps of the IST method but to take into account the perturbation-induced temporal evolution of the scattering data. If we take the breather in the form (19), i.e., a breather at rest, its perturbation-induced dynamics is described by two coupled equations of the first order for the frequency $\omega_{\rm br}$ and the phase χ, and these equations may be obtained in a rather general form,

$$\dot{\omega}_{\rm br} = -\frac{\epsilon}{4} \frac{\sqrt{1-\omega_{\rm br}^2}}{\omega_{\rm br}} D_0 \cos\chi, \tag{A2}$$

$$\dot{\chi} = \omega_{\rm br} + \frac{\epsilon}{4} \frac{\sin\chi}{\sqrt{1-\omega_{\rm br}^2}} \left[D_1 - \frac{1}{\omega_{\rm br}^2} D_0 \right], \tag{A3}$$

where

$$D_n = \int_{-\infty}^{\infty} dz \, \frac{\mathcal{R}(u_{\rm br}(z)) z^n e^z}{\cosh^2 z + a^2}, \quad n = 0,\ 1, \tag{A4}$$

a^2 being defined in Eq. (24). Equations (A2)–(A4) describe evolution of the breather parameters under the influence of a perturbation $\mathcal{R}(u)$, and in the particular case of Eq. (1), Eqs. (A2)–(A4) are transformed to give Eqs. (20)–(23) discussed in Sec. V B.

[1] Yu.S. Kivshar and B.A. Malomed, Rev. Mod. Phys. **61**, 763 (1989).
[2] D.J. Kaup and A.C. Newell, Phys. Rev. B **18**, 5162 (1978).
[3] P.S. Lomdahl and M.R. Samuelsen, Phys. Rev. A **34**, 664 (1986); Phys. Lett. A **128**, 427 (1988).
[4] A.R. Bishop, K. Fesser, P.S. Lomdahl, and S.E. Trullinger, Physica D **7**, 259 (1983).
[5] R. Grauer and B. Birnir, Physica D **56**, 165 (1992).
[6] A.I. Akhiezer, V.G. Bar'yakhtar, and S.V. Peletminsky, *Spin Waves* (Nauka, Moscow, 1967) (English translation: North-Holland, Amsterdam, 1968).
[7] M.M. Bogdan, A.M. Kosevich, and I.V. Manzhos, Fiz. Nizk. Temp. **11**, 991 (1985) [Sov. J. Low Temp. Phys. **11**, 547 (1985)].
[8] C. Vanneste, A. Gilabert, P. Sibillot, and D.B. Ostrowsky, J. Low Temp. Phys. **45**, 517 (1981).
[9] G. Cicogna and L. Fronzoni, Phys. Rev. A **42**, 1901 (1990).
[10] L.D. Landau and E.M. Lifshitz, *Mechanics*, 3rd ed. (Pergamon, New York, 1976).
[11] N. Grønbech-Jensen, Yu.S. Kivshar, and M.R. Samuelsen, Phys. Rev. B **43**, 5698 (1991); **47**, 5013 (1993).
[12] M. Taki, K.H. Spatschek, J.C. Fernandez, R. Grauer, and G. Reinisch, Physica D **40**, 65 (1989).
[13] I.V. Barashenkov, M.M. Bogdan, and V.I. Korobov, Europhys. Lett. **15**, 113 (1991).
[14] H. Pietsch, R. Blaha, E.W. Laedke, and A. Kumar, Europhys. Lett. **15**, 173 (1991).
[15] M. Loève, *Probability Theory* (Van Nostrand, New York, 1965).
[16] J.L. Lumley, *Stochastic Tools in Turbulence* (Academic Press, New York, 1972).
[17] D.W. McLaughlin and A.C. Scott, Phys. Rev. A **18**, 1652 (1978).
[18] A.M. Kosevich and Yu.S. Kivshar, Fiz. Nizk. Temp. **8**, 1270 (1982) [Sov. J. Low Temp. Phys. **8**, 644 (1982)].
[19] V.I. Karpman, E.M. Maslov, and V.V. Solov'ev, Zh. Eksp. Teor. Fiz. **84**, 289 (1983) [Sov. Phys. JETP **57**,

167 (1983)].
[20] O. Legrand and G. Reinisch, Phys. Rev. A **35**, 3522 (1987).
[21] O. Legrand, Phys. Rev. A **36**, 5068 (1987).
[22] R. Boesch and M. Peyrard, Phys. Rev. B **43**, 8491 (1991).
[23] J.G. Caputo and N. Flytzanis, Phys. Rev. A **44**, 6219 (1991).
[24] Yu.S. Kivshar, O.H. Olsen, and M.R. Samuelsen, Phys. Lett. A **168**, 391 (1992).
[25] H. Mikeska, J. Phys. C **11**, 129 (1978).
[26] V.G. Bar'yakhtar, B.A. Ivanov, and A.A. Sukstansky, Zh. Eksp. Teor. Fiz. **78**, 1509 (1980) [Sov. Phys. JETP **51**, 757 (1980)].
[27] R. Sobolewski and C.V. Stancampiano, Phys. Rev. A **31**, 6063 (1985).
[28] D. Ruelle and F. Takens, Commun. Math. Phys. **20**, 167 (1971); S. E. Newhouse, D. Ruelle, and F. Takens, *ibid.*, **64**, 35 (1978).
[29] R.W. Preisendorfer, *Principal Component Analysis in Meteorology and Oceanography* (Elsevier, Amsterdam, 1988).
[30] J.L. Lumley, in *Atmospheric Turbulence and Radio Wave Propagation*, edited by A.M. Yaglom and V.I. Tatarski (Nauka, Moscow, 1967).
[31] N. Aubry, P. Holmes, J.L. Lumley, and E. Stone, J. Fluid Mech. **192**, 115 (1988).
[32] L. Sirovich, in *New Perspectives in Turbulence*, edited by Lawrence Sirovich (Springer, Berlin, 1991).
[33] A.R. Bishop, M. Forest, D.W. McLaughlin, and E.A. Overman II, Physica D **23**, 293 (1986).
[34] G.L. Lamb, *Elements of Soliton Theory* (Wiley, New York, 1979).
[35] M.J. Ablowitz, D.J. Kaup, A.C. Newell, and H. Segur, Phys. Rev. Lett. **30** 1262 (1973).
[36] L.A. Takhatajian and L.D. Fadeev, Theor. Math. Phys. **21**, 1046 (1974).
[37] H.P. McKean, Commun. Pure Appl. Math. **34**, 197 (1981).
[38] E. Date, Osaka J. Math. **19**, 125 (1982).
[39] M.G. Forest and D.W. McLaughlin, J. Math. Phys. **23**, 1248 (1982).